Temperature Model Verification and Beam Characterization on a Solid Target System

S. CHAN[a,1], D. CRYER[a], A.H. ASAD[a,b], R.I. PRICE[a,c]

[a] *Department of Medical Technology and Physics, Sir Charles Gairdner Hospital, Perth, Western Australia*
[b] *Imaging & Applied Physics, Curtin University, Western Australia*
[c] *School of Physics, University of Western Australia, Western Australia*

Introduction

Temperature modeling using Finite Element Analysis (FEA) is widely used by particle beamline designers as a tool to determine the thermal performance of an irradiated target system. A comparison study was performed between FEA calculated temperatures on platinum with experimental results using direct thermocouple measurements. The aims were to determine the best beam model for future solid target design, determine the maximum target current for different target materials and the temperature tolerance for any modification to our existing solid targetry system.

Analysis of the beam spot size and the divergence along the beam line were performed by irradiating glass plates with the primary beam at low target currents. The irradiated plates were analyzed using image processing software to determine the diameter and the stopping range inside the material. The divergence of the beam after it has left the constraint of the cyclotron magnetic field was estimated from the differences in transaxial beam profiles at opposite ends of the beam line. The measured range inside the glass plates was compared to SRIM[3] to determine qualitatively the validity of estimating cyclotron primary beam energy with glass plate irradiation.

Materials and Methods

The theoretical temperature of the target system was determined using SolidWorks 2013 with Flow Simulation Analysis (FSA) module. The FSA module determines the maximum temperature inside the target material given the global conditions (material specification, flow rates, boundary conditions, etc) for a given target current. The proton beam was modeled as a volumetric heat source inside the target material based on the distribution of energy loss in the material along the beam axis. The method used by Čomor, et al[1] was used in this study. The method segmented the target material into five individual layers, each layer being 50 μm thick.

The energy lost per layer was calculated using SRIM[3] and converted into the power loss per layer (Table 1). As calculated, a thickness of 250 μm of platinum completely stops the impinging proton beam at 11.5 MeV with the highest deposition of power per layer corresponding to the Bragg peak.

Target Current (μA)	*Power* (W) Per Layer					*Total Power* (W)
	1	2	3	4	5	
10	18.4	21.1	25.7	40.4	9.41	115
20	36.8	42.2	51.4	80.8	18.8	230
30	55.2	63.3	77.1	121.2	28.2	345
40	73.6	84.4	102.8	161.6	37.6	460
50	92.0	105.5	128.5	201.9	47.0	575

TABLE 1. Power dissipated per layer based on the beam energy lost for different target currents as calculated by SRIM.

The target material used in the simulation reflects the physical target disk used for temperature measurements (platinum, dia. 25.0 mm, thickness 2.0 mm) with two K-type thermocouples (dia. 0.5 mm, stainless steel sheath) embedded inside the platinum disk. One thermocouple is located in the geometric center, while the other is located at a radial position 8mm from center. The outer thermocouple is to determine the peripheral temperature near the o-ring seal. Temperature was maintained below the melting point for the Viton® o-ring (220°C) during the irradiation to ensure the integrity of the water cooling system.

The solid targetry system used in this study is an in-house built, significantly modified version[2] (Fig. 1) of a published design[1].

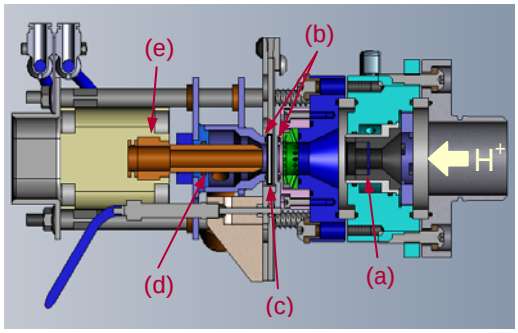

FIGURE 1. Schematic of the Solid Target (a) 10 mm collimator with degrader (b) Viton® O-ring (c) Target material (d) Adjustable water jet (e) 8mm ID water inlet line.

[1]Sun Chan, E-mail: sun.chan@health.wa.gov.au

The solid target system is mounted onto an 18/18 MeV IBA Cyclotron (dual H^- ion source) on the end of a 300 mm beam-line with no internal optics or steering magnets. A graphite collimator reduces the beam to 10 mm in diameter and a degrader is used to reduce the proton beam energy to 11.5 MeV, considered suitable for production of radiometal PET isotopes ^{89}Zr and ^{64}Cu.

Temperature was measured with and without the 300 mm beam-line to compare the effects of beam divergence on the solid target system (Fig. 2 and 3). The temperature at the center and at the radial position was recorded for a range of target currents, 10-50 μA.

FIGURE 2. Solid Target attached to Beam-line.

FIGURE 3. Solid Target with no Beam-line.

The experiment was conducted using both H^- ion sources with different ion-to-puller extraction gaps (ion source 1 is 1.55 mm; ion source 2 is 1.90 mm). The setting of the ion-to-puller gap changes the focusing of the accelerated beam inside the cyclotron cavity.

The cyclotron beam profile as extinguished in a target in three dimensions was measured by placing a square glass plate (80 x 80 x 10 mm) on a custom designed target adapter with no collimator or vacuum window. The main body of the adapter is water cooled (18°C, 14 L/min), while no water cooling is applied to the glass plate itself. The beam was aligned using the platinum disk with the two embedded thermocouples. The glass plates were irradiated at low beam current approximately 10 μA for 8 seconds on the end of the beam-line and directly on the exit port, see figure 4 and figure 5 below.

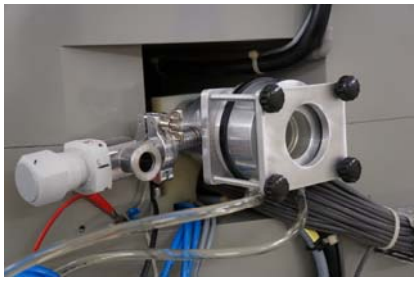

FIGURE 4. Glass plate mounted on Beam-line.

FIGURE 5. Glass plate mounted on exit port.

During the irradiation the exposure of the beam onto the glass plate is monitored via a CCD camera located inside the cyclotron bunker (Fig. 6). Care was taken not to over expose the glass plates to the primary beam to avoid shattering the glass resulting in the loss of cyclotron vacuum. The dose rate of the irradiated glass plates was measured immediately after bombardment and 1 hour post irradiation.

FIGURE 6. View of the solid target from the CCD camera during irradiation.

The irradiated glass plates were scanned on a HP Scanjet 5590 flat bed scanner at 1200 dpi and the images were manipulated using image processing software (ImageJ 1.48v National institute of Health, USA). A standard edge detection method and scaling were applied to images. A multipoint circle fitting tool was used to determine the beam diameter by spatially locating points along the beam edge.

The pixel intensity defining the beam edge was chosen from a series of profile lines drawn across the boundary. The average half max value was determined to be the pixel intensity indicative of the beam edge.

A side profile view of the irradiated glass plates was analysied using the same image processing software to determine the stopping range of the beam inside the material. Calculations in SRIM[3] for various beam energies were aligned with the measured depths for the glass plates. The estimated energy of the primary beam was also compared to the published result by Burrage et al[4].

Results and Discussion

The segmented beam model was used to calculate the temperature on the target surface, and the maximum temperature of the bulk material. The first segment is the leading segment of the material irradiated by the incident proton beam. The results are shown in Table 2 below.

Target Current (μA)	*FEA Model Calculated Temperature* (°C)			
	Bulk Material		8mm Radial Surfaces	
	Max.	Center	Front Surface	Back Surface
10	66	59	27	24
20	110	97	35	29
30	153	132	42	33
40	193	165	49	37
50	233	198	56	41

TABLE 2. Maximum and central temperatures inside the bulk material and at the radial position on the front and back surfaces using segmented beam model.

The temperature measured experiments on the end of a 300 mm beam-line is shown in Table 3 below.

Target Current (μA)	*Measured Temperature* (°C)			
	Ion Source 1		Ion Source 2	
	Center	8mm Radial	Center	8mm Radial
10	84	36	75	34
20	148	48	129	46
30	206	61	180	60
40	278	78	235	73
50	344	93	300	88

TABLE 3. Temperature comparison between Ion sources 1 and 2 with target at the end of the beam-line.

The difference in temperature between ion source 1 and 2 varies from 11°C at 10 μA to 44°C at 50 μA. A smaller variation is observed on the radial position, 2 to 15°C for target current 10 to 50 μA. A smaller ion-to-puller extraction distance (ion source 1) reduces the cross-sectional area of the accelerated beam; the consequent change in beam profile (localized intensity) increases the temperature inside the bulk material for a fixed target current. The highest observed radial temperature was 93°C with a target current of 50 μA using ion source 1. This is well below the melting point for the Viton o-ring seal.

The temperature measured experimentally using the same platinum disk with the beam-line removed is shown in Table 4 below. A maximum temperature difference of 10°C was measured at the center of the platinum material between ion source 1 and 2 when the target is placed at the exit port without the beam-line. While the maximum variation between the ion sources on the radial position is approximately 3°C.

Target Current (μA)	*Measured Temperature* (°C)			
	Ion Source 1		Ion Source 2	
	Center	8mm Radial	Center	8mm Radial
10	68	33	67	33
20	120	43	113	42
30	167	53	156	52
40	211	71	205	68
50	255	89	247	89

TABLE 4. Temperature comparison between Ion source 1 and 2 with target at the exit port.

A comparison between the calculated theoretical and measured temperatures is shown in figures 7 to 10. The temperatures calculated by the FEA model underestimate the temperature regardless of target position or choice of ion source.

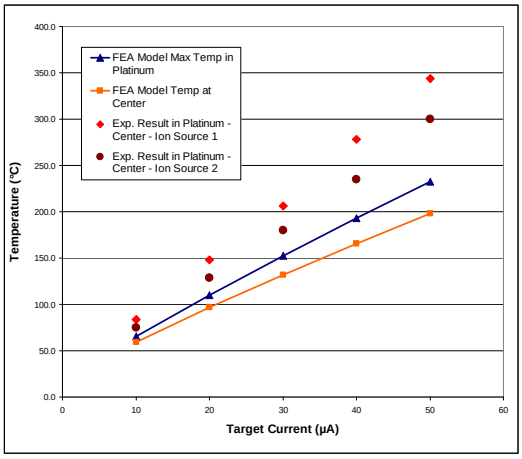

FIGURE 7. Comparison between FEA model and experimental results for the center position on the target attached to the beam-line.

The temperature difference between the FEA model and the experimental results increases with increasing target currents, (Fig. 7). At the target center the FEA model underestimated the temperature by 111°C for ion source 1 and 100°C for ion source 2 at 50μA.

With the target mounted at the exit port the theoretical and measured temperature for the center of the platinum disk is shown in Figure 8 below.

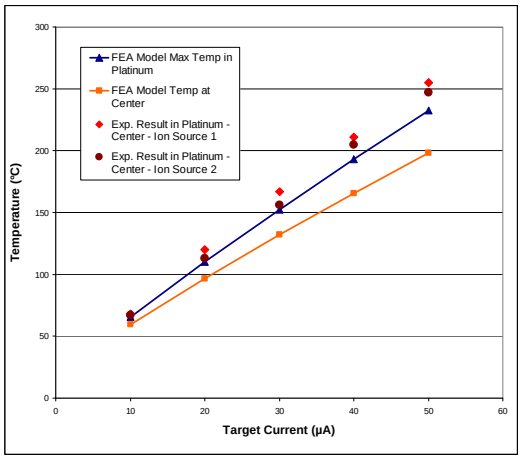

FIGURE 8. Comparison between FEA model and experimental result for the center position on the target measured at the exit port.

The FEA model underestimates the temperature at the center of the platinum disk by 22 to 14°C for ion sources 1 and 2, respectively. As shown with the previous experiment, the margin of error increases with increasing target current.

Comparison between figures 7 and 8 shows the measured temperature at the center of the platinum disk is significantly lower when the target is attached to the exit port of the cyclotron. Difference in beam profile and localised area of high current intensity (hot spots) is undetectable as a change in temperature due to the resolution of the thermocouple. The temperature inside the bulk material is highly dependent on the thermal conductivity of the target material and the proximity of the hot spot to the sensor. The asymmetry of the transaxial beam profile as demonstrated later in this study confirms the effective increase in local intensity when the target is located on the exit port, potentially reducing the ability of the thermocouples to correctly sample the temperature. As observed from this comparative study a noticeable difference in temperature is observed the further the beam travels away from the boundary of the magnetic field of cyclotron due to beam divergence.

With the solid target at the end of the beam-line, target current lost on the collimator and beam-line was >55%. The effect of beam divergence is clearly observed in Table 5 below.

	With Beam-line	No Beam-line
Extracted Current (μA)	119	78.4
Target Current (μA)	50	50
Collimator + Beam-line Current (μA)	68	N/A
Collimator Current (μA)	-	28.7
Current Lost (%)	57%	37%

TABLE 5. Comparison of current lost with and without beam-line. Beam is adjusted so that target current is set at 50 μA for both configurations.

With the target mounted directly at the exit port the current lost was reduced to below 40%. Although the average proton current intensity is the same for any set target current, irrespective of target position, the localized intensity of the beam (due to beam profile) highly influences the temperature measured at the central location. For a fixed target current any loss of beam on the collimator and beam-line places greater reliance on the center of the beam to maintain the same amounts of protons per second impinging on the target surface. In order to compensate for losses along the beam-line a higher output of ions generated in the ion source is required, thus effectively changing the beam cross sectional profile.

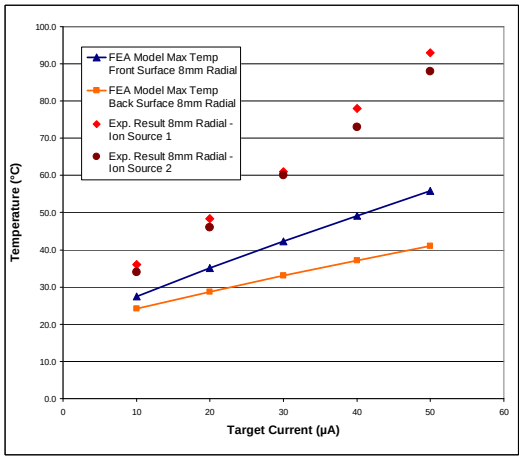

FIGURE 9. Comparison between FEA model and experimental result measured with target on the beam-line for the radial position.

The temperature at the radial position on the beam-line (Fig. 9) observes the same trend as for the temperature measured in the center. The difference between the experimental results and the FEA model is greater for higher target currents.

The FEA model underestimated the temperature by 7 to 37°C for target current of 10 to 50 μA. The error at this location is due partly to the model's assumption of a uniform heat source, applied to the material on a single axis (perpendicular to the material surface) and does not account for any scattering or divergence of the incident proton beam. The temperature at the radial position with the target connected to the exit port is shown in Figure 10 below.

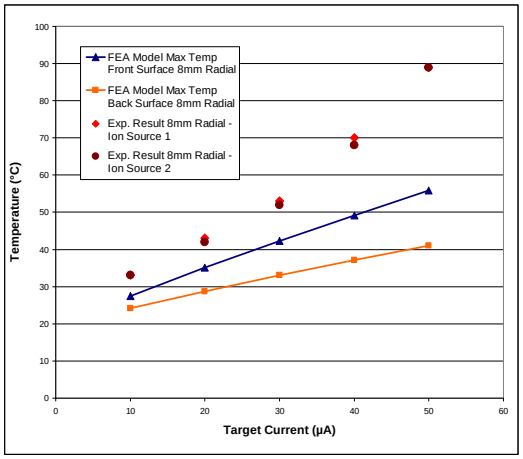

FIGURE 10. Comparison between FEA model and experimental results for the radial position on target attached directly to exit port.

The FEA model underestimated the radial temperature by 6 to 33°C for target current of 10 to 50 μA, for reasons discussed previously. Comparison with figure 9 (target on the beam-line) shows the same margin of error between the FEA and the experimental results, which indicates minimal influence of the proton beam to the radial thermocouple. The 8mm radial position is significantly larger than the collimated beam.

The FEA model underestimated the temperature at the radial location with or without the beam-line and for both ion sources. The difference in temperature between the FEA model and experimental results is due to the assumption that the maximum radial temperature is on the irradiated surface and not inside the material corresponding to the layer with the maximum energy lost (Bragg peak). In addition, the FEA model does not account for the divergence of the proton beam as it travels through the material. Given the temperature at 50μA target current is >90°C (tables 3 and 4) we have capped the experiment below this point to prevent any damage to the o-ring seal.

To illustrate the transaxial beam profile and the range of the beam, its penetration into the glass plate was measured in three-dimensions. Plates were irradiated at low target currents with and without the beam line in place. A dose rate of ~2.0 mSv/hr was measured immediately after irradiation and ~80 μSv/hr at 1 hour post irradiation. After 24 hours the dose rates for the irradiated plates were slightly above background at ~0.7 μSv/hr. A visual inspection of the glass plate showed signs of damage (bubble and micro-fractures) forming in the center of the material and continue to fracture up to several hours post irradiation due to thermal expansion and structural changes (Fig. 11). The fracturing inside the plates subsides once the temperature inside the glass returns to room temperature.

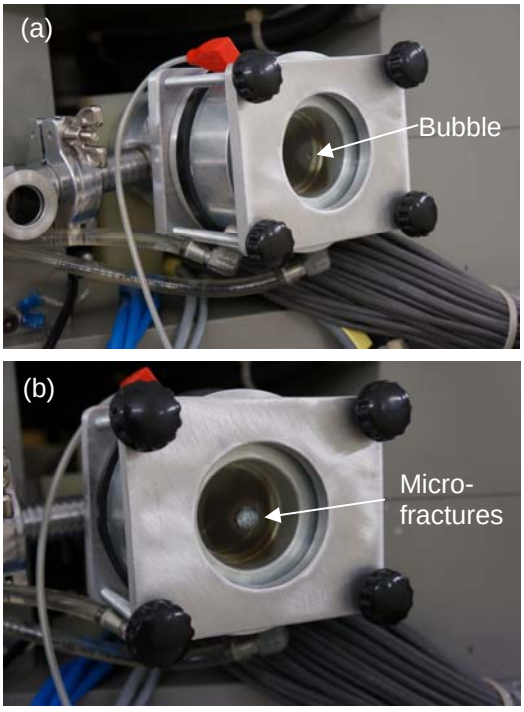

FIGURE 11. Post Irradiation on end of the beam-line for the same glass plate (a) Immediately after bombardment (b) 1 hour after end of bombardment.

The image processing software computes a circle defined by the average diameter determined by edge detection of the transaxial beam profile (Fig. 12c and d). The diameter at the end of the beam line is 16.0 mm, while the diameter without the beam-line is 13.0 mm, therefore the estimated divergence of the beam inside the 300 mm beam-line is 9.5 mrad.

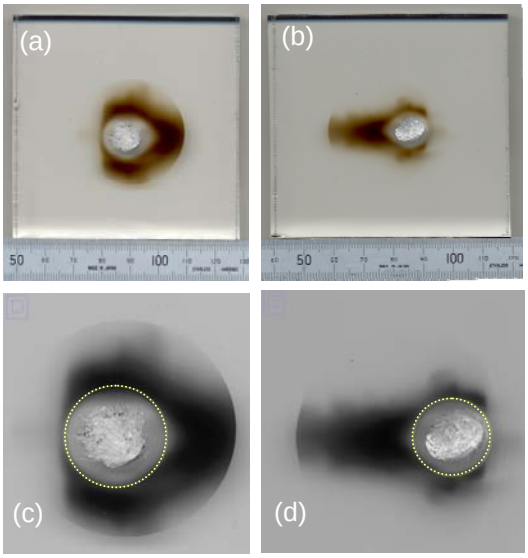

FIGURE 12. Unprocessed images of irradiated glass plates (a) end of the beam-line (b) without the beam-line. Processed images (c) end of the beam-line (d) without the beam-line.

The beam diameter was also estimated using the current measurements in Table 5. Assuming a homogeneous beam collimated to 10 mm with a loss of 57% the un-collimated beam is 15.2 mm, while without the beam-line the un-collimated beam is 12.6 mm (37% beam loss). The calculated divergence using beam current is 8.7 mrad, a difference of 0.8 mrad from the result obtain from the glass plate experiments.

Analysis of the top view of the irradiated glass plates shows the penetration depth of the foot print induced by the beam. Some optical aberration is expected due to the unpolished edges along the glass, thus contributing to the error in depth calculation. The formation of the micro-fractures post irradiation confirms the imprint left in the glass is caused purely by the interaction of proton beam with glass. An estimate of the imprint (not the fractures) inside the glass was measured to be ~1.6 mm (Fig. 13). The stopping range for the measured depth correlates to a primary beam energy of 17.7 MeV in glass (Boro-Silica) using SRIM[3].

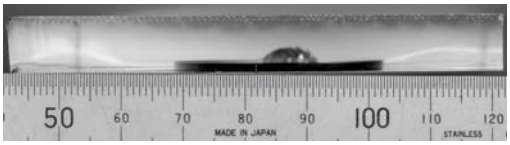

FIGURE 13. Top view of the irradiated glass plates after image processing for beam depth measurement, glass thickness = 10.05 mm.

The result is similar to the norminal beam energy for the cyclotron (~18 MeV) and agrees with the result published by Burrage et al[4].

However, this method provides a qualitative estimate for the beam energy but is limited by the capacity to measure the profile of the Bragg peak from the image.

The imprint left on the glass plates shows an oval shape beam regardless of target location (Fig. 12). A crater has formed on the surface of the irradiated face which indicates some material had vaporized during the irradiation. The visible impact of the beam as it penetrates the glass at normal incidence clearly shows a significant hot spot (represented by fractured glass) surrounded by a darkened annulus representing the true penetration depth of the beam (Fig. 14). The imprint in the material stops flat and the depth of the flat imprint is similar for both experiments with and without the beam-line.

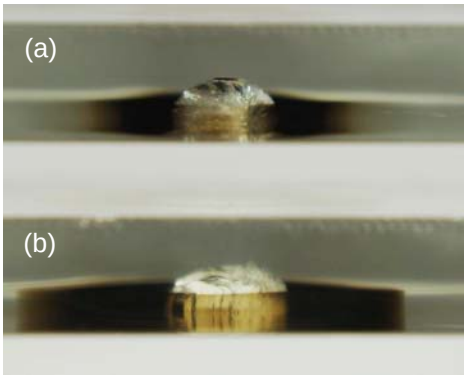

FIGURE 14. Top isometric view (macro photography) of the irradiated glass plates, (a) exit port (b) end of the beam-line

Conclusions

The segmented FEA model was inadequate in determining the temperature for the target at the end of a 300mm beam-line. A combination of beam divergence, beam profile and localized hot spots results in a higher than predicted temperature reading. However, the segmented FEA model provides a good estimation for the temperature observed inside the bulk material when the target is located at the exit port. The segmented FEA model underestimates the temperature at the radial position regardless of ion source or target position.

A comparison between the two ion sources with different ion-to-puller extraction gap, yields minimal temperature difference. Although a difference of 44°C was observed between the two ion sources at the end of the

beam-line, a major contributing factor is beam divergence beyond the magnetic field rather than the beam size of the accelerated beam inside the cyclotron cavity.

Beam spot size measurement using a glass plate is a simple and quick method to verify the beam transaxial profile and energy. The method allows us to quantitatively measure the beam spot size on all exit ports of the cyclotron. A measured beam divergence of 9.5 mrad along the beam-line confirms the significant loss of peripheral beam to the collimator, as per our observation during the temperature experiments.

Further studies are underway to determine the beam hot spots in the irradiated glass plates by using 3D scanners or interferometry of the micro-fractures formed inside the material. Other means of verification using radiographic film can also provide a valuable insight into the beam profile and spot size. In order to avoid micro-fractures a reduced beam current study <5 μA on glass may provide a better beam imprint inside the material for depth measurement. Experiments are underway to polish the glass edges in order avoid any aberrations and reduce the error in beam depth measurement. Energy estimation using the glass technique is a simple and quick guideline measurement, but does not provide the same level of accuracy as the standard stack foil method.

A realistic beam model using the results obtained from the glass plate experiments will improve the FEA simulation for temperature estimation in target material.

Currently the solid target is placed at the end of the beam-line for easy loading and unloading, since multiple target irradiations are performed per month[2]. However, our laboratory is currently developing a new solid targetry system which eliminates the need for a beam-line, potentially resolving the problem with beam divergence and proton current loss. It is estimated that the new target system located at the exit port will be able to sustain a maximum extracted target current of 150μA.

References

1. J. J. Čomor, Z. Stevanovic, M. Rajecevic D. Kosutic: *Nuc. Instrument and Methods in Physics Research Section A,Vol.* **521**, Issue **1**, pp. 161–170, 2004.
2. R.K. Scharli, R.I. Price, S. Chan, D. Cryer, C.M. Jeffery, et al. AIP Conf. Proc. **1509**, 101 (2012); doi: 10.1063/1.4773949.
3. J.F. Ziegler, M.D. Ziegler, J.P. Biersack: *The Stopping and Range of Ion in Matter,* 2012 SRIM code ver. 2012.01
4. J.W. Burrage, A.H. Asad, R.A. Fox, R.I. Price, A.M. Campbell, et al. APESM. Vol. **32**, Issue **2**, pp92-7 2009.

Acknowledgements

The technical and scientific support of the Radiopharmaceutical Production and Development Laboratory (MTP) staff is gratefully acknowledged.